

Constraining properties of anisotropic flow in heavy-ion collisions with multiparticle cumulants

Franco Scarpati, Jerameel

September 23, 2022

Abstract

In heavy ion physics, Quark Gluon Plasma (QGP) is created after a collision. It was shown that its properties can be constrained by the measurements of anisotropic flow. Traditionally anisotropic flow harmonics are estimated by using multivariate cumulants. In this project new multivariate cumulants for anisotropic flow analysis have been introduced, their mathematical and statistical properties have been investigated in detail and tested with carefully designed toy monte carlo studies. These cumulants provide new and independent information about QGP properties when compared to the ones used so far.

14	1 Introduction	3
15	2 Generic Framework	7
16	3 Multiparticle Cumulants	9
17	3.1 Definition	11
18	3.2 Statistical independence.	12
19	3.3 Reduction.	12
20	3.4 Semi-invariance.	12
21	3.5 Homogeneity.	13
22	3.6 Multilinearity.	13
23	3.7 Examples of cumulants	13
24	4 Proposal and demonstration of a new cumulant	16
25	4.1 Statistical independence	17
26	4.2 Reduction	17
27	4.3 Semi-invariance	18
28	4.4 Homogeneity	19
29	4.5 Multilinearity	20
30	5 Toy Monte Carlo studies	20
31	A Demonstrations	25
32	A.1 $\langle \cos [n(\varphi - \Psi_n)] \rangle = v_n$	25
33	A.2 $\langle \cos [n(\varphi_1 - \varphi_2)] \rangle = v_n^2$	25
34	A.3 Two particle correlation	26
35	B Bootstrap technique	26
36	C Code to calculate the correlations	27
37	References	28

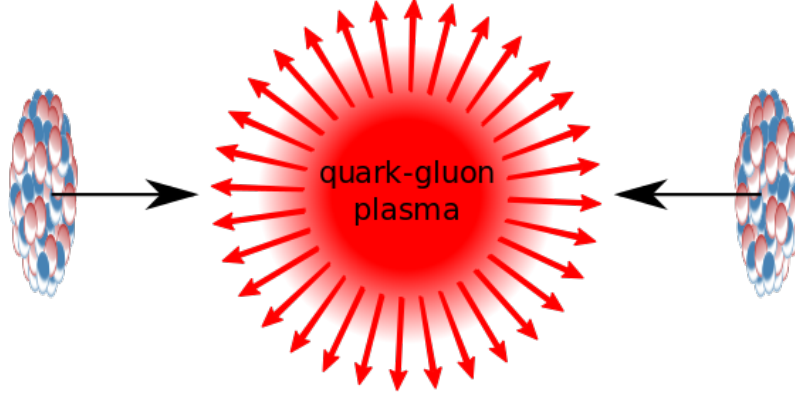


Figure 1: Production of matter at very high temperatures and densities. Two beams of lead nuclei crash to transform in this state. We call it Quark Gluon Plasma and we are looking to describe its behavior. Do we need local interactions and Quantum chromodynamics? or can we study the collective distribution?

1 Introduction

Hadrons are bound states of quarks. Most of the time they appear as mesons (pair quark-antiquark) and baryons (three quarks). If we add energy to mesons, at some point they will decompose producing another meson. We see that at normal conditions (below the Hagedorn temperature of approximately 130-140 MeV), it's impossible to isolate pairs of quarks color-anticolor. This is called color confinement. At hotter conditions this pattern changes, quantum chromodynamics (QCD) predicts that hadrons dissociate to a plasma of quark and gluons (QGP); where they move freely over distances large in comparison to the typical size of a hadron (in the order of fm).

In the QCD phase diagram of Fig. (2) we can see two main regions; the confinement (Hadron gas) and deconfinement (QGP). The boundary area between these two is a topic of current research and it can be either a smooth crossover, or phase transition of first or second order. For instance, in the last decades, new studies describing its expected characteristics emerged; the phase coexistence and location of a hypothetical critical point [7]. Astrophysicists find the conditions which existed in the region at low temperatures and high chemical potential μ_B , the conditions which can be found in the core of neutron stars. Matter inside them exhibits characteristics of the deconfined phase, which is interpreted as evidence for the presence of quark-matter cores [6]. At the upper left, region of high temperatures and low μ_B , we find the conditions just few microseconds after the Big Bang. Early universe was filled with QGP, then went through a smooth transition to the confinement (under 175 MeV).

Physicists produce QGP at colliders. High energy heavy ion collisions create a fireball that reaches the QGP region and simulates the early universe. Used nuclei must have large mass and energies, because their product has the sufficient density and temperature to become QGP. Momenta and energies of resulting particles in a magnetic field are then detected and so the reconstruction of QGP, as it expands and cools, can be done. In 2000, the first production of QGP was announced at CERN; the Super Proton Synchrotron (SPS) fired very-high-energy beams of lead ions into gold or lead targets. Collisions created temperatures 100,000 times hotter than the centre of the Sun, and the highest energy densities (3–4 GeV per cubic femtometer) [8]. The contemporary experiment is ALICE; it was specifically designed as a dedicated heavy-ion experiment, with the primary goal to

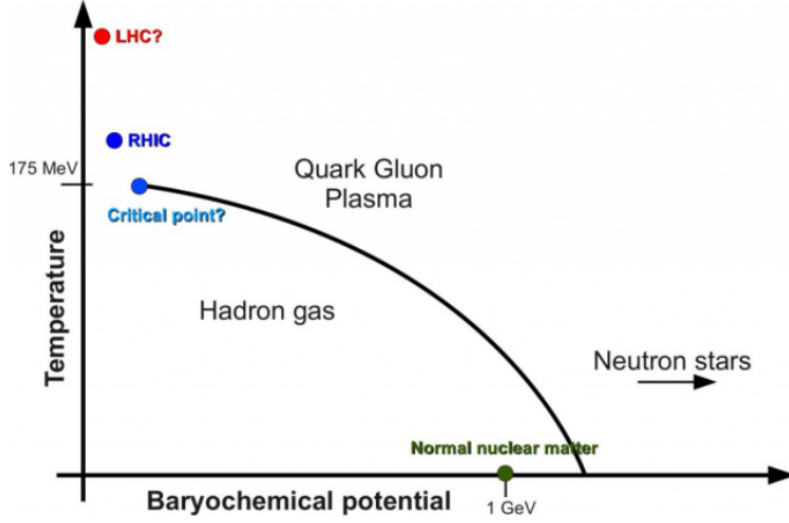


Figure 2: Phase diagram of Quantumchromodynamics. We distinguish two main areas; the hadronic and Quark gluon plasma regions. In the first only exists pairs quark-antiquark (confinement), in the second quarks and gluons move freely over distances typical of a size of a hadron [2].

69 analyse the QGP. Fig. (3) shows the detector layout.

70 Describing QGP with only QCD is very difficult; one needs to solve the non-linearity
 71 of the gluon interaction, the strong coupling, the dynamical many body system and con-
 72 finement. Surprisingly, QGP behaves like an almost perfect liquid [9]. This constraints the
 73 QCD; we don't need long scattering formulas to describe particle interactions anymore; we
 74 surpass this challenge by using effective theories, like viscous hydrodynamics. As conse-
 75 quence of it we can describe QGP with the macroscopic thermodynamic properties, such
 76 as the equation of state (EoS), temperature and order of the phase transition, transport
 77 coefficients and so on. We need then the transport coefficients such as shear viscosity η ,
 78 bulk viscosity ζ , heat conductivity λ , etc. Let's take a look to the equation of state:

$$P = (e, n) \quad (1)$$

79 which expresses the pressure P as a function of energy density e and baryon density n . We
 80 obtain it by doing numerical simulations of QCD on the lattice. It does not only describe
 81 expansion and collective flow of matter but also provides important information in the
 82 intermediate stage for other phenomena.

83 In non-central heavy-ion collisions the initial volume of the interacting system is anisotropic
 84 in coordinate space (see Fig. 4). The general characteristic of a flow is that any anisotropy
 85 in the coordinate space also transforms in the momentum space; moving a bottle of water
 86 will move it's molecules and change their momentum, while moving a bottle of gas will do
 87 generally nothing, it remains isotropic. Quarks and Gluons play here the role of molecules
 88 in QGP. Clearly, this is an indirect probe of the viscosity.

89 The first important focus of this paper is to describe the probability density function
 90 (p.d.f) of the transmitted anisotropy in momentum space $f(\varphi)$. We can always start doing
 91 the most general expansion, a Fourier series:

$$f(\varphi) = \int_0^{2\pi} \frac{1}{2\pi} \left[1 + 2 \sum_{n=1}^{\infty} v_n \cos[n(\varphi - \Psi_n)] \right] \quad (2)$$

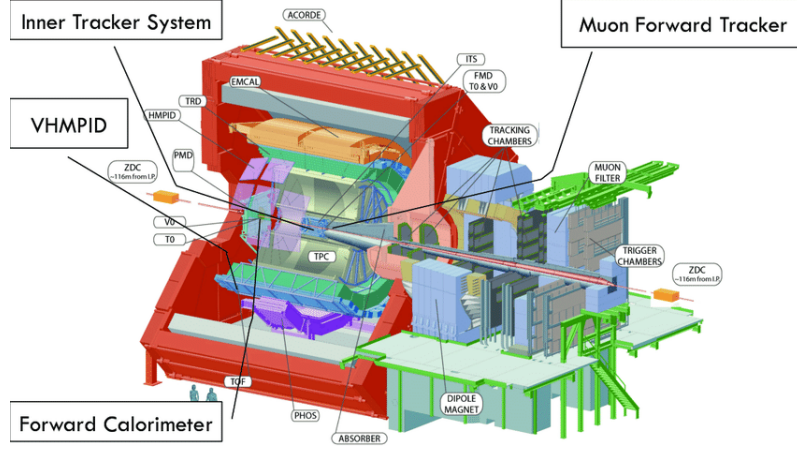


Figure 3: Schematic description of the ALICE experiment. Collision happens at the center of the cylinder (Inner tracking system). For more information about the components see the paper [15].

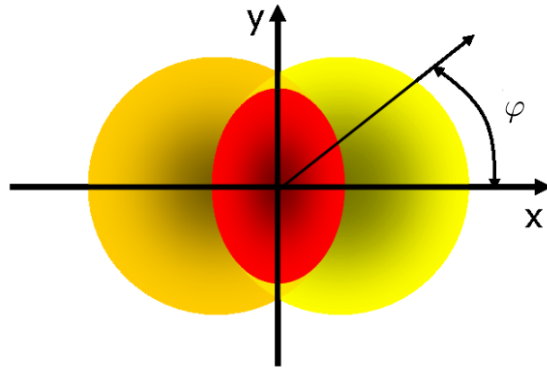


Figure 4: Coordinate space anisotropy of the initial volume of the interacting system (red) created in heavy-ion collisions [2].

where φ is the azimuthal angle whose sample space is the interval $[0, 2\pi)$, v_n are anisotropic flow harmonics and Ψ_n corresponding symmetry planes. v_n determines the form of distribution; v_1 is directed, v_2 elliptic and v_3 triangular flow. Due to the collision geometry, the dominant harmonic in non-central collisions is the elliptic flow v_2 . It quantifies how the system responds to the initial spatial ellipsoidal anisotropy. In this project we considerate up to eight harmonics.

Mathematically can be demonstrated that v_n has the following equivalence (Appendix A.1):

$$v_n = \langle \cos [n(\varphi - \Psi_n)] \rangle \quad (3)$$

Where the average value of function $a(x)$ is defined the following way:

$$\langle a(x) \rangle \equiv \int_0^{2\pi} a(x) f(x) dx \quad (4)$$

Eq. (3) includes also harmonic symmetry planes Ψ_n , that are different in every event, and can be difficult to detect at colliders, only easily measurable quantities, are the angles and momenta.

If anisotropic flow is the dominant source of correlations among produced particles at a collision, they are emitted independently and are only correlated to a common symmetry plane. This is why we can factorize the joint p.d.f. for any number of particles n into a product of individual p.d.f's $f_{\varphi_i}(\varphi_i)$, that have the same form of Eq. (2):

$$f(\varphi_1, \dots, \varphi_n) = f_{\varphi_1}(\varphi_1) \dots f_{\varphi_n}(\varphi_n) \quad (5)$$

Of course with adding more particles and multiplying their p.d.f to the joint p.d.f. one can find the correlation of a very large number of them.

Two-particle azimuthal correlation is the simplest one and can be expressed as the square of flow harmonics (Appendix A.2):

$$\langle \cos [n(\varphi_1 - \varphi_2)] \rangle = v_n^2 \quad (6)$$

The main problem of Eq. (6) is that the two azimuthal angles φ_1 and φ_2 must be different, otherwise there are trivial contributions from self-correlations, which are large and equal to 1. We can solve this using nested loop algorithms; calculating the correlation of first particle relative to each one of the rest, then doing the same for second particle and so on. Obviously this is not an efficient way, takes too much time for a computer to calculate all the loops and it's impossible with the amount of particles created in heavy-ion collisions. We can avoid this, if we calculate the Q-vector evaluated in harmonic n , Q_n , that by definition only needs one pass over all particles, and if we find formulas for particle correlations that can be expressed in terms of Q-vectors.

$$Q_n \equiv \sum_{i=1}^M e^{in\varphi_i} . \quad (7)$$

φ_i is the azimuthal angle of the i -particle, and M is the number of particles. The key point is that all multi-particle azimuthal correlations can be expressed analytically in terms of Q -vectors evaluated (in general) different harmonics. For example the two particle correlation is now (Appendix A.3):

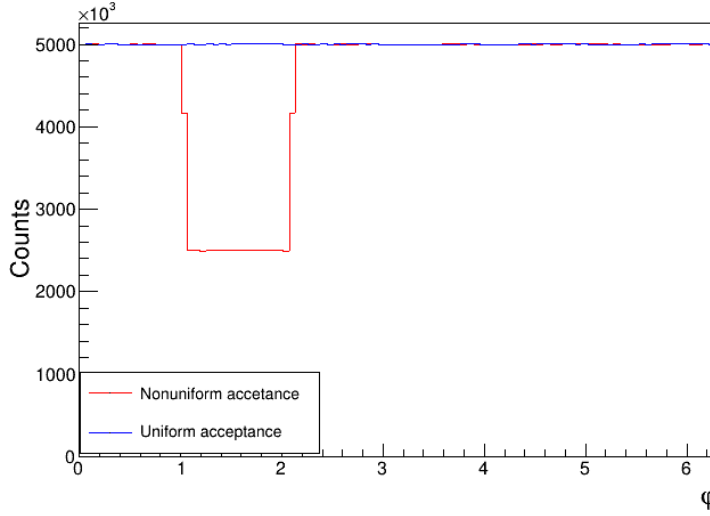


Figure 5: Simulating a detector that have bias in the azimuth angles between 30 and 60°, making them 50% less probable (red histogram). Here we compare this with the uniform acceptance (blue histogram).

$$\begin{aligned}
\langle 2 \rangle &\equiv \langle \cos(n(\varphi_1 - \varphi_2)) \rangle \\
&= \frac{1}{\binom{M}{2} 2!} \sum_{\substack{i,j=1 \\ (i \neq j)}}^M e^{in(\varphi_i - \varphi_j)} \\
&= \frac{1}{\binom{M}{2} 2!} [|Q_n|^2 - M]
\end{aligned} \tag{8}$$

125 Despite the efficiency of a single pass, finding higher order correlation formulas in
126 terms of Q-vectors became very complicated. Four, five and six correlations will gradually
127 have way longer expressions. One clever way to avoid them is using recursion algorithms;
128 the seventh and higher correlations can be calculated in terms of the lower order ones
129 recursively [4].

130 2 Generic Framework

131 In this chapter we introduce a framework to simulate Pb-Pb collisions and calculate par-
132 ticle correlations using computational algorithms. Later in chapter 5, we explore our new
133 proposed cumulant with the help of this framework.

134 At the LHC, azimuthal angles can be measured with high precision. New correlation
135 techniques use them to estimate the flow amplitudes v_n and the symmetry planes Ψ_n . For
136 instance, the connection between these three is described in the following formula [3]:

$$\left\langle e^{i(n_1\varphi_1 + \dots + n_m\varphi_m)} \right\rangle = v_{n_1} \dots v_{n_m} e^{i(n_1\Psi_{n_1} + \dots + n_m\Psi_{n_m})}, \tag{9}$$

137 The average goes over all distinct tuples of m different azimuthal angles φ reconstructed
138 in the same event. A set n_1, \dots, n_m consists of m non-zero integers. In each event,
139 measuring symmetry planes alone is very problematic, that's why we want to eliminate

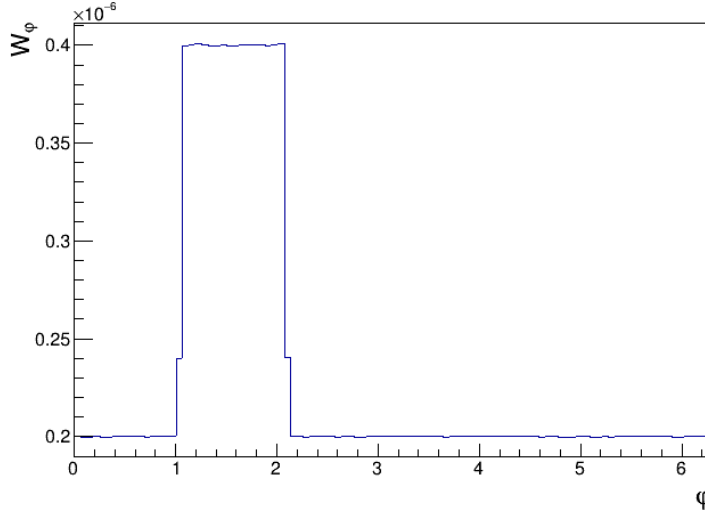


Figure 6: Weights obtained inverting the histogram of nonuniform acceptance from Fig. (2). We don't need to normalize it because the definition in Eq. (11) does it for us.

140 their contribution. In the case of an idealized geometry, all symmetry planes Ψ_n coincide.
 141 If we carefully choose the values in this set, (e.g. by taking value of each integer equal
 142 number of times with positive and negative sign), we can then discard the contribution. In
 143 other words, since the impact parameter orientation is uncontrolled, the only non-trivial
 144 correlations must have azimuthal symmetry [3]:

$$n_1 + \dots + n_k = 0. \quad (10)$$

145 Real detection of particle-collisions has some degree of inefficiency. To solve this, we
 146 introduce particle weights and we get a new definition for the average m-particle correlation
 147 in harmonics n_1, n_2, \dots, n_m :

$$\begin{aligned} \langle m \rangle_{n_1, n_2, \dots, n_m} &\equiv \left\langle e^{i(n_1 \varphi_1 + n_2 \varphi_2 + \dots + n_m \varphi_m)} \right\rangle \\ &\equiv \frac{\sum_{\substack{k_1, k_2, \dots, k_m=1 \\ k_1 \neq k_2 \neq \dots \neq k_m}}^M w_{k_1} w_{k_2} \dots w_{k_m} e^{i(n_1 \varphi_{k_1} + n_2 \varphi_{k_2} + \dots + n_m \varphi_{k_m})}}{\sum_{\substack{k_1, k_2, \dots, k_m=1 \\ k_1 \neq k_2 \neq \dots \neq k_m}}^M w_{k_1} w_{k_2} \dots w_{k_m}}. \end{aligned} \quad (11)$$

148 M is the multiplicity of an event, φ labels the azimuthal angles of the produced particles
 149 and w particle weights. The condition removes all possible autocorrelations. Weights
 150 compensate, for example, bias in azimuthal angle that the detector can have. Theoretically,
 151 if we have the following values of flow harmonics,

$$v_n = 0.04 + n \cdot 0.01, n = 1, 2, \dots, 6. \quad (12)$$

152 and if we use Eq. (9), then we find theoretical value for each multiparticle azimuthal
 153 correlation of interest.

154 To prove our generic framework using weights, we did a toy Monte Carlo simulation for
 155 a nonuniform acceptance with just half the probability to get a particle within the azimuth
 156 range 30 and 60°.

157 Firstly we selected the harmonics that resulted in the following input values:

$$\begin{aligned}
 \langle 2 \rangle &\equiv \langle 2 \rangle_{-2,2} = v_2^2 = 3.6 \times 10^{-3}, \\
 \langle 3 \rangle &\equiv \langle 3 \rangle_{-5,-1,6} = v_1 v_5 v_6 = 4.5 \times 10^{-4}, \\
 \langle 4 \rangle &\equiv \langle 4 \rangle_{-3,-2,2,3} = v_2^2 v_3^2 = 1.764 \times 10^{-5}, \\
 \langle 5 \rangle &\equiv \langle 5 \rangle_{-5,-4,3,3,3} = v_3^3 v_4 v_5 = 2.4696 \times 10^{-6}, \\
 \langle 6 \rangle &\equiv \langle 6 \rangle_{-2,-2,-1,-1,3,3} = v_1^2 v_2^2 v_3^2 = 4.41 \times 10^{-8}, \\
 \langle 7 \rangle &\equiv \langle 7 \rangle_{-6,-5,-1,1,2,3,6} = v_1^2 v_2 v_3 v_5 v_6^2 = 9.45 \times 10^{-9}, \\
 \langle 8 \rangle &\equiv \langle 8 \rangle_{-6,-6,-5,2,3,3,4,5} = v_2 v_3^2 v_4 v_5^2 v_6^2 = 1.90512 \times 10^{-9}.
 \end{aligned} \tag{13}$$

158 We assumed 10^6 events. In each one of them the reaction plane Ψ_{RP} was uniformly sampled
 159 in the interval $[0, 2\pi]$, then 500 azimuth angles from the following p.d.f:

$$f(\varphi) = \frac{1}{2\pi} \left[1 + 2 \sum_{n=1}^6 v_n \cos[n(\varphi - \Psi_{RP})] \right] \tag{14}$$

160 With this, we did two runs over events to fill two histograms, which will play the role of
 161 nonuniform and uniform acceptances, respectively. In Fig. (2) we compared both. As
 162 we see here, for the filling of first one we forced additionally 0.5 probability to get angles
 163 between 30 and 60°. Weights were then obtained inverting this histogram (Fig. 6). Note
 164 that the definition in Eq. (11) don't need normalized weights.

165 Next step was the calculation of correlations. For the first six we used standalone
 166 formulas and for the seventh and eighth recursion techniques. These algorithms were
 167 obtained in the paper [4]. We did 3 runs. The first for uniform acceptance, second for the
 168 nonuniform acceptance and third the nonuniform acceptance that considers weights. Each
 169 run had 10^6 events. In each event we got angles from the p.d.f of Eq. (14) and reaction
 170 plane from uniform distribution. Then, we calculated Q vector and correlations. The final
 171 results were averages over all events. Fig. (7) shows the 2,3,4,5,6,7 and 8 correlations.
 172 Clearly the use of weights like in Eq. (9) corrects values from the nonuniform acceptance,
 173 thus solving azimuthal bias in detectors.

174 3 Multiparticle Cumulants

175 Up to now we were only handling statistically independent particles. But we want to
 176 isolate genuine multiparticle correlations, from multiparticle correlations which are just
 177 a trivial superposition of few-particle correlations. That's why we use cumulants. This
 178 was first proposed by Borghini et. al. [10] at the turn of the Millenium. The work was
 179 very influential and changed the way anisotropic flow analysis is performed in high-energy
 180 physics. Cumulants will provide less biased estimators true harmonics v_n . For instance,
 181 the simplest multivariate cumulant can be defined as:

$$\langle X_1 X_2 \rangle_c = \langle X_1 X_2 \rangle - \langle X_1 \rangle \langle X_2 \rangle. \tag{15}$$

182 One important fundamental property of cumulants is described in theorem 1 from the
 183 paper of Kubo [1], and we interpret it as follows:

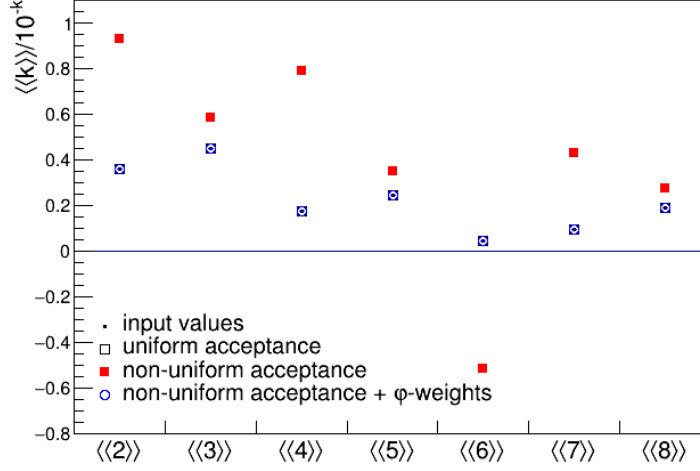


Figure 7: Results showing the correlations using harmonics of Eq. (13). As we see here, the use of weights (non-uniform acceptance + weights, blue dots) corrects the azimuthal bias of detectors (non-uniform acceptance, red dots). For a better view, k-correlation values were divided by 10^{-k} .

1. non-vanishing multi-particle cumulant is equivalent to the existence of genuine multi-body interaction;
2. if there is no genuine multi-body interaction, then the corresponding multi-particle cumulant is identically zero;
3. however, if multi-particle cumulant is identically zero, that does NOT mean that there is no genuine multi-body interaction => cumulant can also be trivially zero, due to underlying symmetries.

In the past decade physicists took many multivariate estimators as cumulants, but sadly most of them were found to be incorrect. Last year, the first strict mathematical formalism was published by Bilandzic et. al. [12]. In this section we will summarize them.

It is clear that we need first a mathematical notation to refer our cumulants, and study their properties using it. In each event we have a set of N stochastic variables X_1, \dots, X_N and we would like to find the corresponding multivariate p.d.f. $f(X_1, \dots, X_N)$, because it gives information of all statistical properties. Experimentally in our colliders, it is very difficult to determine these p.d.f's. Instead of a long computational calculation, we use multivariate moments μ and cumulants κ . With them we save time. In this paper we will take in consideration the following notation:

$$\mu_{\nu_1, \dots, \nu_N} \equiv \mu(X_1^{\nu_1}, \dots, X_N^{\nu_N}) \equiv \langle X_1^{\nu_1}, \dots, X_N^{\nu_N} \rangle \quad (16)$$

$$\kappa_{\nu_1, \dots, \nu_N} \equiv \kappa(X_1^{\nu_1}, \dots, X_N^{\nu_N}) \equiv \langle X_1^{\nu_1}, \dots, X_N^{\nu_N} \rangle_c \quad (17)$$

The subindice ν_i , where i is at least 1 and at most N , in the first term, determines the order of variable X_i . For example ν_1 is the order of the variable X_1 . When we define the moments, we don't specify the type; they are not necessarily the azimuthal moments in a non-uniform acceptance, like in our generic framework. In the most general way the statistical moment is defined the following way:

$$\mu_{\nu_1, \dots, \nu_N} \equiv \int X_1^{\nu_1} \cdots X_N^{\nu_N} f(X_1, \dots, X_N) dX_1 \cdots dX_N \quad (18)$$

Of course, we would need the p.d.f. if we just use this definition. But in this paper we calculate correlations from our toy Monte Carlo simulations, so we can avoid this integrals and just use Eq. (16).

3.1 Definition

The definition of multivariate moments $\mu_{\nu_1, \dots, \nu_N}$ in Eq. (16) can be rewritten very compactly in terms of the moment generating function, $M(\xi_1, \dots, \xi_N)$, which is defined as,

$$M(\xi_1, \dots, \xi_N) = \left\langle e^{\sum_{j=1}^N \xi_j X_j} \right\rangle \quad (19)$$

We can do a Taylor expansion of the exponential function in auxiliary variables ξ_1, \dots, ξ_N about zero, replace all averages of X_1, \dots, X_N with $\mu_{\nu_1, \dots, \nu_N}$ [see Eq. (16)], and obtain all multivariable moments $\mu_{\nu_1, \dots, \nu_N}$ as coefficients of different orders in auxiliary variables ξ_1, \dots, ξ_N :

$$M(\xi_1, \dots, \xi_N) = \sum_{\nu_1, \dots, \nu_N} \left(\prod_j \frac{\xi_j^{\nu_j}}{\nu_j!} \right) \mu_{\nu_1, \dots, \nu_N} \quad (20)$$

where all indices ν_1, \dots, ν_N run from zero. The multivariate moments can therefore be obtained directly from their generating function with the following standard expression:

$$\mu_{\nu_1, \dots, \nu_N} = \left. \frac{\partial^{\nu_1}}{\partial \xi_1^{\nu_1}} \cdots \frac{\partial^{\nu_N}}{\partial \xi_N^{\nu_N}} M(\xi_1, \dots, \xi_N) \right|_{\xi_1 = \xi_2 = \dots = \xi_N = 0} \quad (21)$$

The generating function for cumulants, $K(\xi_1, \dots, \xi_N)$, is defined in terms of the moment generating function:

$$K(\xi_1, \dots, \xi_N) \equiv \ln M(\xi_1, \dots, \xi_N) = \ln \left\langle e^{\sum_{j=1}^N \xi_j X_j} \right\rangle \quad (22)$$

By definition, multivariate cumulants $\kappa_{\nu_1, \dots, \nu_N}$ are coefficients in the formal Taylor expansion of their generating function $K(\xi_1, \dots, \xi_N)$ about zero:

$$K_{\nu_1, \dots, \nu_N} = \sum_{\nu_1, \dots, \nu_N} \left(\prod_j \frac{\xi_j^{\nu_j}}{\nu_j!} \right) \kappa_{\nu_1, \dots, \nu_N} \quad (23)$$

In the sum $\sum_{\nu_1, \dots, \nu_N}$, the term $\nu_1 = \dots = \nu_N = 0$ was excluded from summation. Analogously to moments, cumulants can be obtained directly from their generating function:

$$\kappa_{\nu_1, \dots, \nu_N} = \left. \frac{\partial^{\nu_1}}{\partial \xi_1^{\nu_1}} \cdots \frac{\partial^{\nu_N}}{\partial \xi_N^{\nu_N}} K(\xi_1, \dots, \xi_N) \right|_{\xi_1 = \xi_2 = \dots = \xi_N = 0} \quad (24)$$

The details of underlying multivariate p.d.f. $f(X_1, \dots, X_N)$ can be estimated equivalently either with moments or with cumulants, because from relation of Eq. (17), it can be shown that all cumulants $\kappa_{\nu_1, \dots, \nu_N}$ can be uniquely expressed in terms of moments $\mu_{\nu_1, \dots, \nu_N}$, and vice versa. We are easily measurable moments with the average $\langle X_1^{\nu_1} \cdots X_N^{\nu_N} \rangle$, while cumulants $\langle X_1^{\nu_1} \cdots X_N^{\nu_N} \rangle_c$ are obtained with multiparticle calculations, like in our toy

monte carlo section. In practice, one first measures moments, then in the next step calculates cumulants from them, and finally from cumulants draws the physics conclusions and constraints on the many-body problem in question.

After clarifying notation and definitions, we can finally introduce the general properties. Here we take them as sufficient requirements; when a multivariate mathematical expression satisfy all of them then it is a cumulant. It is not clear if there are more properties, that is a subject of new studies. In any case, with the properties of this paper, physicists can discard many wrongly consider multivariate cumulants of flow amplitudes. The detailed proof of all properties can be found in Appendix A 3 from the paper of Bilandzic et. al. [12].

3.2 Statistical independence.

A multivariate cumulant $\kappa_{\nu_1, \dots, \nu_N} \equiv \langle X_1^{\nu_1}, \dots, X_N^{\nu_N} \rangle_c$ is identically zero if its stochastic variables X_1, \dots, X_N can be divided into two groups which are statistically independent. This implies that the cumulant is zero if at least one of its variables is statistically independent from the rest. When some group of variables are correlated, then their cumulant can be nonzero.

3.3 Reduction.

If in a set of variables X_1, \dots, X_N two or more are identical, the resulting cumulant has lower number of variables; we can group them and add their indices:

$$\kappa_{\nu_1, \dots, \nu_N} = \left\langle X_1^{\nu_1} \cdots X_N^{\nu_N} \right\rangle_c = \left\langle X_1^{\tilde{\nu}_1} \cdots X_M^{\tilde{\nu}_M} \right\rangle_c = \kappa_{\tilde{\nu}_1, \dots, \tilde{\nu}_M}, \quad (25)$$

where $\tilde{\nu}_i$ is the sum of indices of all variables which are equal to X_i . Clearly $M \leq N$.

For example, if we have the set X_1, X_2, X_3, X_4 and X_1 is equal to X_2 , then we can convert the cumulant $\kappa_{\nu_1, \nu_2, \nu_3, \nu_4}$ and conclude:

$$\kappa_{\nu_1, \nu_2, \nu_3, \nu_4} = \left\langle X_1^{\nu_1} X_2^{\nu_2} X_3^{\nu_3} X_4^{\nu_4} \right\rangle_c = \left\langle X_1^{\nu_1 + \nu_2} X_3^{\nu_3} X_4^{\nu_4} \right\rangle_c = \kappa_{\nu_1 + \nu_2, \nu_3, \nu_4} \quad (26)$$

The four variate cumulant became a three variate cumulant. Similarly, if we choose to equalize all variables in the set X_1, \dots, X_N to X , then the final expression is a univariate cumulant of X of order $\nu_1 + \dots + \nu_N$:

$$\kappa_{\nu_1, \dots, \nu_N} = \left\langle X_1^{\nu_1} \cdots X_N^{\nu_N} \right\rangle_c = \left\langle X^{\nu_1 + \dots + \nu_N} \right\rangle_c = \kappa_{\nu_1 + \dots + \nu_N} \quad (27)$$

We can further assume that the orders of all variables are equal to 1, $\nu_1 = \nu_2 = \dots = \nu_N = 1$, then the original multivariate cumulant of N random variables reduces to the N th-order univariate cumulant, i.e., $\kappa_{1, \dots, 1} = \kappa_N$.

3.4 Semi-invariance.

We will see what happens if we sum constants to each variable in the set X_1, \dots, X_N . If the sum of indices in the multivariate cumulant $\kappa_{\nu_1, \dots, \nu_N}$ is equal or bigger than 2, then it follows that adding constants c_i , where $1 \leq i \leq N$, won't change the original cumulant:

$$\kappa([X_1 + c_1]^{\nu_1}, \dots, [X_N + c_N]^{\nu_N}) = \kappa(X_1^{\nu_1}, \dots, X_N^{\nu_N}) = \kappa_{\nu_1, \dots, \nu_N}. \quad (28)$$

262 In the case that one variable is equal to 1 and the rest to zero, then adding a constant to
 263 that variable has the same effect that adding the constant to the original cumulant:

$$\kappa(1, \dots, 1, X_i + c_i, 1, \dots, 1) = c_i + \kappa(1, \dots, 1, X_i, 1, \dots, 1). \quad (29)$$

264 For the univariate case, this property will made all cumulants shift-invariant, i.e., for any
 265 constant c ,

$$\kappa[(X + c)^\nu] = \kappa(X^\nu), \quad (30)$$

266 where ν is equal or bigger than 2. Last case is the first-order cumulant; this will add the
 267 constant to the cumulant:

$$\kappa(X + c) = c + \kappa(X). \quad (31)$$

268 3.5 Homogeneity.

269 A mathematical expression will be a multivariate cumulant of flow amplitudes, if and only if
 270 multiplying constants c_i to each variable X_i will result in the original cumulant multiplied
 271 by the product of all constants, where $1 \leq i \leq N$. This is called the homogeneity of
 272 cumulants. For instance, if we have a set of variables X_1, \dots, X_N and a cumulant $\kappa_{\nu_1, \dots, \nu_N}$,
 273 then the following expression must be true:

$$\kappa[(c_1 X_1)^{\nu_1}, \dots, (c_N X_N)^{\nu_N}] = c_1^{\nu_1} \dots c_N^{\nu_N} \kappa(X_1^{\nu_1}, \dots, X_N^{\nu_N}) = c_1^{\nu_1} \dots c_N^{\nu_N} \kappa_{\nu_1, \dots, \nu_N}. \quad (32)$$

274 For the univariate case, this requirement reduces to

$$\kappa([cX]^\nu) = c^\nu \kappa(X^\nu) \quad (33)$$

275 3.6 Multilinearity.

276 A mathematical expression is a multivariate cumulant of flow amplitudes, if and only if
 277 the following is true. When we have a set of variables Z_1, \dots, Z_N and one of the variables
 278 is linear (of order 1), let's say X_1 , if we express it as a sum of other M statistical variables
 279 $\sum_{i=1}^M X_i$, then the resulting cumulant is the sum of cumulants with each variable X_i as
 280 first variable:

$$\kappa\left[\left(\sum_{i=1}^M X_i\right), Z_2^{\nu_2}, \dots, Z_N^{\nu_N}\right] = \sum_{i=1}^M \kappa[X_i, Z_2^{\nu_2}, \dots, Z_N^{\nu_N}] \quad (34)$$

281 We can see here that the rest of variables can be linear or not ($\nu_i > 1$). For the univariate
 282 case we have:

$$\kappa\left(\sum_{i=1}^M X_i\right) = \sum_{i=1}^M \kappa(X_i), \quad (35)$$

283 wich is a linear univariate estimator.

284 3.7 Examples of cumulants

285 From the definition of Eq. (16), (17) and Taylor series, we can express the first cumulants
 286 in terms of the moments, although, in this paper, we will focus more in the verification of

287 cumulants.

$$\begin{aligned}
\kappa_1 &= \mu_1, \\
\kappa_2 &= \mu_2 - \mu_1^2, \\
\kappa_{1,1} &= \mu_{1,1} - \mu_{0,1}\mu_{1,0}, \\
\kappa_{2,1} &= 2\mu_{0,1}\mu_{1,0}^2 - 2\mu_{1,1}\mu_{1,0} - \mu_{0,1}\mu_{2,0} + \mu_{2,1}, \\
\kappa_{1,2} &= 2\mu_{1,0}\mu_{0,1}^2 - 2\mu_{1,1}\mu_{0,1} - \mu_{0,2}\mu_{1,0} + \mu_{1,2}, \\
\kappa_{1,1,1} &= 2\mu_{0,0,1}\mu_{0,1,0}\mu_{1,0,0} - \mu_{0,1,1}\mu_{1,0,0} - \mu_{0,1,0}\mu_{1,0,1} - \mu_{0,0,1}\mu_{1,1,0} + \mu_{1,1,1}. \quad (36)
\end{aligned}$$

288 Having well defined properties, we can continue to illustrate examples of true multivari-
289 ate cumulants of flow amplitudes. With these examples we will improve our understanding
290 and will be able to recognize a true cumulant. This will help us in the next section, where
291 a new and original multivariate cumulant is proposed and demonstrated. On this paper
292 we will only handle square of flow amplitudes as stochastic variables.

293 Let's begin with the easiest two particle cumulant of Eq. (15). The stochastic variables
294 are chosen to be $X_1 \equiv v_m^2$ and $X_2 \equiv v_n^2$.

295 • **Statistical independence** Like we already did in the beginning of the section, by
296 definition this cumulant is zero if the two variables are statistically independent.

$$\langle X_1 X_2 \rangle_c = \langle X_1 X_2 \rangle - \langle X_1 \rangle \langle X_2 \rangle = 0 \quad (37)$$

297 • **Reduction** If we have that $X_1 = X_2 = X = v^2$ then it follows:

$$\begin{aligned}
\langle X_1 X_2 \rangle_c &= \langle X X \rangle - \langle X \rangle \langle X \rangle = \langle X^2 \rangle - \langle X \rangle^2 \\
&= \langle v^4 \rangle - \langle v^2 \rangle^2 \quad (38)
\end{aligned}$$

298 wich is an univariate cumulant κ_2 (Appendix B of [12]).

299 • **Semi-invariance** Adding two constants c_1 and c_2 will have the following effect:

$$\begin{aligned}
\langle (X_1 + c_1)(X_2 + c_2) \rangle_c &= \langle (v_m^2 + c_1)(v_n^2 + c_2) \rangle - \langle (v_m^2 + c_1) \rangle \langle (v_n^2 + c_2) \rangle \\
&= \langle (v_m^2 v_n^2 + v_m^2 c_2 + c_1 v_n^2 + c_1 c_2) \rangle \\
&\quad - \langle (v_m^2 + c_1) \rangle \langle (v_n^2 + c_2) \rangle \\
&= \langle v_m^2 v_n^2 \rangle + c_2 \langle v_m^2 \rangle + c_1 \langle v_n^2 \rangle + c_1 c_2 \\
&\quad - (\langle v_m^2 \rangle + c_1)(\langle v_n^2 \rangle + c_2) \\
&= \langle v_m^2 v_n^2 \rangle + c_2 \langle v_m^2 \rangle + c_1 \langle v_n^2 \rangle + c_1 c_2 \\
&\quad - \langle v_m^2 \rangle \langle v_n^2 \rangle - c_1 \langle v_n^2 \rangle - c_2 \langle v_m^2 \rangle - c_1 c_2 \\
&= \langle v_m^2 v_n^2 \rangle - \langle v_m^2 \rangle \langle v_n^2 \rangle = \langle X_1 X_2 \rangle_c, \quad (39)
\end{aligned}$$

300 which does not change anything, as expected for a true cumulant.

301 • **Homogeneity** Now we multiply the variables v_m^2 and v_n^2 with the constants c_1 and c_2 ,
302 respectively:

$$\begin{aligned}
\langle (c_1 X_1)(c_2 X_2) \rangle_c &= \langle (c_1 v_m^2)(c_2 v_n^2) \rangle - \langle c_1 v_m^2 \rangle \langle c_2 v_n^2 \rangle \\
&= c_1 c_2 (\langle v_m^2 v_n^2 \rangle - \langle v_m^2 \rangle \langle v_n^2 \rangle) \\
&= c_1 c_2 \langle X_1 X_2 \rangle_c \quad (40)
\end{aligned}$$

303 and see that the homogeneity is satisfied.

304 • **Multilinearity** Let's take the first variable $X_1 = v_m^2$ as linear. When it is the sum
 305 of other two variables $v_m^2 = z_1^2 + z_2^2$, where $Z_1 = z_1^2$ and $Z_2 = z_2^2$, then the expression
 306 becomes:

$$\begin{aligned}
 \langle (Z_1 + Z_2)X_2 \rangle_c &= \langle (z_1^2 + z_2^2)v_n^2 \rangle_c \equiv \langle (z_1^2 + z_2^2)v_n^2 \rangle - \langle (z_1^2 + z_2^2) \rangle \langle v_n^2 \rangle \\
 &= \langle z_1^2 v_n^2 \rangle + \langle z_2^2 v_n^2 \rangle - (\langle z_1^2 \rangle \langle v_n^2 \rangle + \langle z_2^2 \rangle \langle v_n^2 \rangle) \\
 &= \langle z_1^2 v_n^2 \rangle - \langle z_1^2 \rangle \langle v_n^2 \rangle + \langle z_2^2 v_n^2 \rangle - \langle z_2^2 \rangle \langle v_n^2 \rangle \\
 &= \langle Z_1 X_2 \rangle_c + \langle Z_2 X_2 \rangle_c
 \end{aligned} \tag{41}$$

307 Symmetric cumulants of flow amplitudes are defined by $SC(k, l) \equiv \langle v_k^2 v_l^2 \rangle - \langle v_k^2 \rangle \langle v_l^2 \rangle$,
 308 with the angular brackets denoting an average over all events. In recent studies it was found
 309 that different $SC(k, l)$ observables provide new and independent constraints for both the
 310 initial conditions and the QGP properties. For instance, It was showed that the different
 311 $SC(k, l)$ observables have different sensitivities to the initial conditions of a heavy-ion
 312 collision and properties of the created system, and can therefore help in separating the
 313 effects of η/s in the final state anisotropies from the contributions originating in the initial
 314 state. Furthermore, it was demonstrated that the SC observables are more sensitive to the
 315 temperature dependence $\eta/s(T)$ than the individual flow amplitudes, which are sensitive
 316 only to the average values $\langle \eta/s \rangle$ [11]. Asymmetric cumulants (ACs), on the other hand,
 317 only differ with SCs that the even exponents are not equal. Let's continue with an AC,
 318 because it has the same type of our new cumulant from the next section:

$$AC_{2,1}(m, n) = \langle v_m^4 v_n^2 \rangle - \langle v_m^4 \rangle \langle v_n^2 \rangle - 2 \langle v_m^2 v_n^2 \rangle \langle v_m^2 \rangle + 2 \langle v_m^2 \rangle^2 \langle v_n^2 \rangle \tag{42}$$

319 Here the subindices 2, 1 mean that the flow amplitudes v_m^2 and v_n^2 are elevated to the
 320 maximal exponents 2 and 1, respectively. We are proceeding now to prove that it is a
 321 cumulant.

322 • **Statistical independence** If the fluctuations v_n^2 and v_m^2 are completely uncorrelated,
 323 then Eq. (42) becomes

$$AC_{2,1}(m, n) = \langle v_m^4 \rangle \langle v_n^2 \rangle - \langle v_m^4 \rangle \langle v_n^2 \rangle - 2 \langle v_m^2 \rangle \langle v_n^2 \rangle \langle v_m^2 \rangle + 2 \langle v_m^2 \rangle^2 \langle v_n^2 \rangle = 0, \tag{43}$$

324 as expected in absence of genuine correlations between the two variables.

325 • **Reduction** Again, if we set the two flow amplitudes equal to the same quantity $v_m^2 =$
 326 $v_n^2 = v^2$ then we have

$$\begin{aligned}
 AC_{2,1}(m, n) &= \langle v^6 \rangle - \langle v^4 \rangle \langle v^2 \rangle - 2 \langle v^4 \rangle \langle v^2 \rangle + 2 \langle v^2 \rangle^2 \langle v^2 \rangle \\
 &= \langle v^6 \rangle - 3 \langle v^4 \rangle \langle v^2 \rangle + 2 \langle v^2 \rangle^3.
 \end{aligned} \tag{44}$$

327 This is a valid univariate cumulant with v^2 as fundamental variable, κ_3 from the paper
 328 of Bilandzic et. al. [12].

329 • **Semi-invariance** We will add now two constants c_1 and c_2 to the variables X_1 and

330 X_2 , respectively. Let's see if this property is fulfilled.

$$\begin{aligned}
\langle (v_m^2 + c_m)^2 (v_n^2 + c_n) \rangle_c &= \langle (v_m^2 + c_m)^2 (v_n^2 + c_n) \rangle - \langle (v_m^2 + c_m)^2 \rangle \langle (v_n^2 + c_n) \rangle \\
&\quad - 2 \langle (v_m^2 + c_m) (v_n^2 + c_n) \rangle \langle v_m^2 + c_m \rangle \\
&\quad + 2 \langle v_m^2 + c_m \rangle^2 + \langle v_n^2 + c_n \rangle \\
&= \langle (v_m^4 + 2c_m v_m^2 + c_m^2) (v_n^2 + c_n) \rangle \\
&\quad - \langle v_m^4 + 2c_m v_m^2 + c_m^2 \rangle \langle v_n^2 + c_n \rangle \\
&\quad - 2 \langle v_m^2 v_n^2 + c_m v_n^2 + c_n v_m^2 + c_m c_n \rangle \langle v_m^2 + c_m \rangle \\
&\quad + 2 (\langle v_m^2 \rangle^2 + 2c_m \langle v_m^2 \rangle + c_m) \langle v_n^2 + c_n \rangle \\
&= AC_{2,1}(m, n) \\
&\quad + 2c_m (\langle v_m^2 v_n^2 \rangle - 2 \langle v_m^2 \rangle \langle v_n^2 \rangle - \langle v_m^2 v_n^2 \rangle + \\
&\quad 2 \langle v_m^2 \rangle \langle v_n^2 \rangle) \\
&\quad + c_n (\langle v_m^4 \rangle - \langle v_m^4 \rangle 2 \langle v_m^2 \rangle^2 - 2 \langle v_m^2 \rangle^2) \\
&\quad + c_m^2 (3 \langle v_n^2 \rangle - 3 \langle v_n^2 \rangle) + 2c_m c_n (3 \langle v_m^2 \rangle - 3 \langle v_m^2 \rangle) \\
&\quad + c_m^2 c_n (3 - 3) \\
&= AC_{2,1}(m, n)
\end{aligned} \tag{45}$$

331 As expected, the cumulant won't change when adding constants.

332 • **Homogeneity** Let's multiply the constants c_m and c_n to the variables v_m^2 and v_n^2 ,
333 respectively:

$$\begin{aligned}
\langle (c_m v_m^2)^2 (c_n v_n^2) \rangle_c &= \langle c_m^2 v_m^4 c_n v_n^2 \rangle - \langle c_m^2 v_m^4 \rangle \langle c_n v_n^2 \rangle - 2 \langle c_m v_m^2 c_n v_n^2 \rangle \langle c_m v_m^2 \rangle \\
&\quad + 2 \langle c_m v_m^2 \rangle^2 \langle c_n v_n^2 \rangle \\
&= c_m^2 c_n AC_{2,1}(m, n).
\end{aligned} \tag{46}$$

334 As we see here, homogeneity is valid for our expression $AC_{2,1}(m, n)$.

335 • **Multilinearity** We consider now the second variable linear, so we have three variables,
336 v_m^2 , v_n^2 and v_k^2 . Let's see if our expression $AC_{2,1}(m, n)$ is linear:

$$\begin{aligned}
AC_{2,1}(m, n + k) &= \langle v_m^4 (v_n^2 + v_k^2) \rangle - \langle v_m^4 \rangle \langle v_n^2 + v_k^2 \rangle - 2 \langle v_m^2 (v_n^2 + v_k^2) \rangle \langle v_m^2 \rangle \\
&\quad + 2 \langle v_m^2 \rangle \langle v_n^2 + v_k^2 \rangle \\
&= AC_{2,1}(m, n) + AC_{2,1}(m, k).
\end{aligned} \tag{47}$$

337 And yes, it is, so our expression shows multilinearity.

338 We have just desmostrated that the expression $AC_{2,1}(m, n)$ given by Eq. (42) is a valid
339 multivariate cumulant with v_m^2 and v_n^2 being the fundamental stochastic variables. After
340 all this long examples we have now a clear understanding of cumulants and can proceed
341 to analyse our new cumulant.

342 4 Proposal and demonstration of a new cumulant

343 In this section we have taken the asymmetric cumulant of flow amplitudes $AC_{3,1}(m, n)$
344 from the paper of Bilandzic et. al. (Eq. 38 in [12]), and we will show that this a proper
345 cumulant that meets all the requirements from section 3. By definition, it can probe the

genuine correlations between the different moments, 3 and 1, of different flow harmonics v_m^2 and v_n^2 , respectively. Therefore, it has access to new and independent information to constrain different stages in the heavy-ion evolution. The multivariate estimator has following form:

$$\begin{aligned}
AC_{3,1}(m, n) &= \langle v_m^6 v_n^2 \rangle - \langle v_m^6 \rangle \langle v_n^2 \rangle - 3 \langle v_m^2 v_n^2 \rangle \langle v_m^4 \rangle - 3 \langle v_m^4 v_n^2 \rangle \langle v_m^2 \rangle \\
&\quad + 6 \langle v_m^4 \rangle \langle v_m^2 \rangle \langle v_n^2 \rangle + 6 \langle v_m^2 v_n^2 \rangle \langle v_m^2 \rangle^2 - 6 \langle v_m^2 \rangle^3 \langle v_n^2 \rangle \\
&= \langle X_1^3 X_2 \rangle_c
\end{aligned} \tag{48}$$

We now demonstrate with the detailed calculus that this observable satisfies all fundamental mathematical properties of cumulants. The first stochastic variable is $X_1 = v_m^2$ and the second $X_2 = v_n^2$.

4.1 Statistical independence

Let's begin with the easiest one. Statistical independence means that the mean of a products is equal to the product of the mean of its factors. We see in the following expression that when the variables are independent to each other then the asymmetric cumulant becomes zero:

$$\begin{aligned}
AC_{3,1}(m, n) &= \langle v_m^6 \rangle \langle v_n^2 \rangle - \langle v_m^6 \rangle \langle v_n^2 \rangle - 3 \langle v_m^2 \rangle \langle v_n^2 \rangle \langle v_m^4 \rangle - 3 \langle v_m^4 \rangle \langle v_n^2 \rangle \langle v_m^2 \rangle \\
&\quad + 6 \langle v_m^4 \rangle \langle v_m^2 \rangle \langle v_n^2 \rangle + 6 \langle v_m^2 \rangle \langle v_n^2 \rangle \langle v_m^2 \rangle^2 - 6 \langle v_m^2 \rangle^3 \langle v_n^2 \rangle \\
&= 0.
\end{aligned} \tag{49}$$

4.2 Reduction

Now we go to the second property. To prove the reduction we need to equalize the two variables, $X_1 = X_2 = v^2$. Then Eq. (48) becomes:

$$\begin{aligned}
AC_{3,1}(m, n) &= \langle v^6 v^2 \rangle - \langle v^6 \rangle \langle v^2 \rangle - 3 \langle v^2 v^2 \rangle \langle v^4 \rangle - 3 \langle v^4 v^2 \rangle \langle v^2 \rangle \\
&\quad + 6 \langle v^4 \rangle \langle v^2 \rangle \langle v^2 \rangle + 6 \langle v^2 v^2 \rangle \langle v^2 \rangle^2 - 6 \langle v^2 \rangle^3 \langle v^2 \rangle \\
&= \langle v^8 \rangle - \langle v^6 \rangle \langle v^2 \rangle - 3 \langle v^4 \rangle^2 - 3 \langle v^6 \rangle \langle v^2 \rangle \\
&\quad + 6 \langle v^4 \rangle \langle v^2 \rangle^2 + 6 \langle v^4 \rangle \langle v^2 \rangle^2 - 6 \langle v^2 \rangle^3 \langle v^2 \rangle \\
&= \langle v^8 \rangle - 4 \langle v^6 \rangle \langle v^2 \rangle - 3 \langle v^4 \rangle^2 + 12 \langle v^4 \rangle \langle v^2 \rangle^2 - 6 \langle v^2 \rangle^4 \\
&= \kappa_4.
\end{aligned} \tag{50}$$

κ_4 is a univariate cumulant as mentioned in Appendix B from the paper of Bilandzic et. al. [12]. Thus we have reduced our two-variate cumulant to the valid univariate cumulant and proved this property.

364 4.3 Semi-invariance

365 In Eq. (48) we add two constants c_1 and c_2 to the squared flow amplitudes v_m^2 and v_n^2 ,
 366 respectively. If the cumulant does not change, then the semi-invariance is fulfilled.

$$\begin{aligned}
 AC_{3,1}(m, n) = & \langle (v_m^2 + c_1)^3 (v_n^2 + c_2) \rangle - \langle (v_m^2 + c_1)^3 \rangle \langle v_n^2 + c_2 \rangle \\
 & + 3 \langle (v_m^2 + c_1)(v_n^2 + c_2) \rangle \langle (v_m^2 + c_1)^2 \rangle \\
 & - 3 \langle (v_m^2 + c_1)^2 (v_n^2 + c_2) \rangle \langle v_m^2 + c_1 \rangle \\
 & + 6 \langle (v_m^2 + c_1)^2 \rangle \langle v_m^2 + c_1 \rangle \langle v_n^2 + c_2 \rangle \\
 & + 6 \langle (v_m^2 + c_1)(v_n^2 + c_2) \rangle \langle v_m^2 + c_1 \rangle^2 - 6 \langle v_m^2 + c_1 \rangle^3 \langle v_n^2 + c_2 \rangle
 \end{aligned} \tag{51}$$

367 Expressions inside the parentheses on each term can be expanded.

$$\begin{aligned}
 AC_{3,1}(m, n) = & \langle (v_m^6 + 3v_m^4 c_1 + 3v_m^2 c_1^2 + c_1^3)(v_n^2 + c_2) \rangle \\
 & - \langle (v_m^6 + 3v_m^4 c_1 + 3v_m^2 c_1^2 + c_1^3) \rangle \langle (v_n^2 + c_2) \rangle \\
 & - 3 \langle (v_m^2 v_n^2 + v_m^2 c_2 + c_1 v_n^2 + c_1 c_2) \rangle \langle (v_m^4 + 2v_m^2 c_1 + c_1^2) \rangle \\
 & - 3 \langle (v_m^4 + 2v_m^2 c_1 + c_1^2)(v_n^2 + c_2) \rangle \langle v_m^2 + c_1 \rangle \\
 & + 6 \langle (v_m^4 + 2v_m^2 c_1 + c_1^2) \rangle \langle v_m^2 + c_1 \rangle \langle v_n^2 + c_2 \rangle \\
 & + 6 \langle (v_m^2 v_n^2 + v_m^2 c_2 + c_1 v_n^2 + c_1 c_2) \rangle \langle v_m^2 + c_1 \rangle^2 \\
 & - 6 \langle v_m^2 + c_1 \rangle^3 \langle v_n^2 + c_2 \rangle
 \end{aligned} \tag{52}$$

368 If we expand further, we obtain the next long expression. Here by definition we can
 369 express the average of a sum as the sum of averages, and the average of a variable multiplied
 370 with a constant as the product constant and average. For a better view all terms appear
 371 on the position of their ancestor product from Eq. (52).

$$\begin{aligned}
AC_{3,1}(m, n) = & \langle v_m^6 v_n^2 \rangle + 3c_1 \langle v_m^4 v_n^2 \rangle + 3c_1^2 \langle v_m^2 v_n^2 \rangle + c_1^3 \langle v_n^2 \rangle \\
& + c_2 \langle v_m^6 \rangle + 3c_1 c_2 \langle v_m^4 \rangle + 3c_1^2 c_2 \langle v_m^2 \rangle + c_1^3 c_2 \\
& - \langle v_m^6 \rangle \langle v_n^2 \rangle - 3c_1 \langle v_m^4 \rangle \langle v_n^2 \rangle - 3c_1^2 \langle v_m^2 \rangle \langle v_n^2 \rangle - c_1^3 \langle v_n^2 \rangle \\
& - c_2 \langle v_m^6 \rangle - 3c_1 c_2 \langle v_m^4 \rangle - 3c_1^2 c_2 \langle v_m^2 \rangle - c_1^3 c_2 \\
& - 3 \langle v_m^2 v_n^2 \rangle \langle v_m^4 \rangle - 3c_2 \langle v_m^2 \rangle \langle v_m^4 \rangle - 3c_1 \langle v_n^2 \rangle \langle v_m^4 \rangle - 3c_1 c_2 \langle v_m^4 \rangle \\
& - 6c_1 \langle v_m^2 v_n^2 \rangle \langle v_m^2 \rangle - 6c_1 c_2 \langle v_m^2 \rangle^2 - 6c_1^2 \langle v_n^2 \rangle \langle v_m^2 \rangle - 6c_1^2 c_2 \langle v_m^2 \rangle \\
& - 3c_1^2 \langle v_m^2 v_n^2 \rangle - 3c_2 c_1^2 \langle v_m^2 \rangle - 3c_1^3 \langle v_n^2 \rangle - 3c_1^3 c_2 \\
& - 3 \langle v_m^4 v_n^2 \rangle \langle v_m^2 \rangle - 6c_1 \langle v_m^2 v_n^2 \rangle \langle v_m^2 \rangle - 3c_1^2 \langle v_n^2 \rangle \langle v_m^2 \rangle - 3c_2 \langle v_m^4 \rangle \langle v_m^2 \rangle \\
& - 6c_1 c_2 \langle v_m^2 \rangle^2 - 3c_1^2 c_2 \langle v_m^2 \rangle - 3c_1 \langle v_m^4 v_n^2 \rangle - 6c_1^2 \langle v_m^2 v_n^2 \rangle \\
& - 3c_1^3 \langle v_n^2 \rangle - 3c_1 c_2 \langle v_m^4 \rangle - 6c_1 c_2 \langle v_m^2 \rangle - 3c_1^3 c_2 \\
& + 6 \langle v_m^4 \rangle \langle v_m^2 \rangle \langle v_n^2 \rangle + 12c_1 \langle v_m^2 \rangle^2 \langle v_n^2 \rangle + 6c_1 \langle v_m^2 \rangle \langle v_n^2 \rangle + 6c_1 \langle v_m^4 \rangle \langle v_n^2 \rangle \\
& + 12c_1^2 \langle v_m^2 \rangle \langle v_n^2 \rangle + 6c_1^3 \langle v_n^2 \rangle + 6c_2 \langle v_m^4 \rangle \langle v_m^2 \rangle + 12c_1 c_2 \langle v_m^2 \rangle^2 \\
& + 6c_1 c_2 \langle v_m^2 \rangle + 6c_1 c_2 \langle v_m^4 \rangle + 12c_1^2 c_2 \langle v_m^2 \rangle + 6c_1^3 c_2 \\
& + 6 \langle v_m^2 v_n^2 \rangle \langle v_m^2 \rangle^2 + 6c_2 \langle v_m^2 \rangle \langle v_m^2 \rangle^2 + 6c_1 \langle v_n^2 \rangle \langle v_m^2 \rangle^2 + 6c_1 c_2 \langle v_m^2 \rangle^2 \\
& + 12c_1 \langle v_m^2 v_n^2 \rangle \langle v_m^2 \rangle + 12c_1 c_2 \langle v_m^2 \rangle \langle v_m^2 \rangle + 12c_1^2 \langle v_n^2 \rangle \langle v_m^2 \rangle + 12c_1^2 c_2 \langle v_m^2 \rangle \\
& + 6c_1^2 \langle v_m^2 v_n^2 \rangle + 6c_1^2 c_2 \langle v_m^2 \rangle + 6c_1^3 \langle v_n^2 \rangle + 6c_1^3 c_2 \\
& - 6 \langle v_m^2 \rangle^3 \langle v_n^2 \rangle - 18 \langle v_m^2 \rangle^2 \langle v_n^2 \rangle - 18c_1^2 \langle v_m^2 \rangle \langle v_n^2 \rangle - 6c_1^3 \langle v_n^2 \rangle \\
& - 6c_2 \langle v_m^2 \rangle^3 - 18c_2 \langle v_m^2 \rangle^2 - 18c_1^2 c_2 \langle v_m^2 \rangle - 6c_1^3 c_2
\end{aligned} \tag{53}$$

372 We can separate the terms that does not have our introduced constants c_1 and c_2 .
 373 As consequence we see that all this terms form the original expression $AC_{3,1}(m, n)$ from
 374 Eq. (48). With a long and exhausting calculation by hand, we can check that the rest
 375 terms sum zero. This means that $AC_{3,1}(m, n)$ hasn't changed after adding constants to its
 376 variables, the semi-invariance is proven.

377 4.4 Homogeneity

378 We will multiply each squared flow amplitude v_m^2 and v_n^2 by the constants c_1 and c_2 ,
 379 respectively. As we see in the following expression, the original estimator $AC_{3,1}(m, n)$ only
 380 changes by a new factor $c_1^3 c_2$, thus proving the homogeneity.

$$\begin{aligned}
AC_{3,1}(m, n) = & \langle (c_1 v_m^2)^3 (c_2 v_n^2) \rangle - \langle (c_1 v_m^2)^3 \rangle \langle c_2 v_n^2 \rangle \\
& - 3 \langle (c_1 v_m^2) (c_2 v_n^2) \rangle \langle (c_1 v_m^2)^2 \rangle - 3 \langle (c_1 v_m^2)^2 (c_2 v_n^2) \rangle \langle (c_1 v_m^2) \rangle \\
& + 6 \langle (c_1 v_m^2)^2 \rangle \langle (c_1 v_m^2) \rangle \langle (c_2 v_n^2) \rangle + 6 \langle (c_1 v_m^2) (c_2 v_n^2) \rangle \langle (c_1 v_m^2) \rangle^2 \\
& - 6 \langle (c_1 v_m^2) \rangle^3 \langle (c_2 v_n^2) \rangle \\
= & c_1^3 c_2 \langle v_m^6 v_n^2 \rangle - c_1^3 c_2 \langle v_m^6 \rangle \langle v_n^2 \rangle - 3c_1^3 c_2 \langle v_m^2 v_n^2 \rangle \langle v_m^4 \rangle - 3c_1^3 c_2 \langle v_m^4 v_n^2 \rangle \langle v_m^2 \rangle \\
& + 6c_1^3 c_2 \langle v_m^4 \rangle \langle v_m^2 \rangle \langle v_n^2 \rangle + 6c_1^3 c_2 \langle v_m^2 v_n^2 \rangle \langle v_m^2 \rangle^2 - 6c_1^3 c_2 \langle v_m^2 \rangle^3 \langle v_n^2 \rangle \\
= & c_1^3 c_2 AC_{3,1}(m, n).
\end{aligned} \tag{54}$$

381 4.5 Multilinearity

382 In our asymmetric estimator $AC_{3,1}(m, n)$, the second stochastic variable is linear. We can
 383 express it as the sum of two squared flow amplitudes $v_n^2 + v_k^2$. The following form is taken:

$$\begin{aligned} AC_{3,1}(m, n+k) = & \langle v_m^6(v_n^2 + v_k^2) \rangle - \langle v_m^6 \rangle \langle (v_n^2 + v_k^2) \rangle - 3 \langle v_m^2(v_n^2 + v_k^2) \rangle \langle v_m^4 \rangle \\ & - 3 \langle v_m^4(v_n^2 + v_k^2) \rangle \langle v_m^2 \rangle + 6 \langle v_m^4 \rangle \langle v_m^2 \rangle \langle (v_n^2 + v_k^2) \rangle \\ & + 6 \langle v_m^2(v_n^2 + v_k^2) \rangle \langle v_m^2 \rangle^2 - 6 \langle v_m^2 \rangle^3 \langle (v_n^2 + v_k^2) \rangle \end{aligned} \quad (55)$$

384 We can proceed to solve the averages and express everything in terms of correlations.

$$\begin{aligned} AC_{3,1}(m, n+k) = & \langle v_m^6 v_n^2 \rangle + \langle v_m^6 v_k^2 \rangle - \langle v_m^6 \rangle \langle v_n^2 \rangle - \langle v_m^6 \rangle \langle v_k^2 \rangle - 3 \langle v_m^2 v_n^2 \rangle \langle v_m^4 \rangle \\ & - 3 \langle v_m^2 v_k^2 \rangle \langle v_m^4 \rangle - 3 \langle v_m^4 v_n^2 \rangle \langle v_m^2 \rangle - 3 \langle v_m^4 v_k^2 \rangle \langle v_m^2 \rangle \\ & + 6 \langle v_m^4 \rangle \langle v_m^2 \rangle \langle v_n^2 \rangle + 6 \langle v_m^4 \rangle \langle v_m^2 \rangle \langle v_k^2 \rangle + 6 \langle v_m^2 v_n^2 \rangle \langle v_m^2 \rangle^2 \\ & + 6 \langle v_m^2 v_k^2 \rangle \langle v_m^2 \rangle^2 - 6 \langle v_m^2 \rangle^3 \langle v_n^2 \rangle - 6 \langle v_m^2 \rangle^3 \langle v_k^2 \rangle \end{aligned} \quad (56)$$

385 If we separate the terms with v_n^2 from the ones with v_k^2 , then we get the sum of two
 386 estimators, $AC_{3,1}(m, n)$ and $AC_{3,1}(m, k)$. This proves the multilinearity.

$$\begin{aligned} AC_{3,1}(m, n+k) = & \langle v_m^6 v_n^2 \rangle - \langle v_m^6 \rangle \langle v_n^2 \rangle - 3 \langle v_m^2 v_n^2 \rangle \langle v_m^4 \rangle - 3 \langle v_m^4 v_n^2 \rangle \langle v_m^2 \rangle \\ & + 6 \langle v_m^4 \rangle \langle v_m^2 \rangle \langle v_n^2 \rangle + 6 \langle v_m^2 v_n^2 \rangle \langle v_m^2 \rangle^2 - 6 \langle v_m^2 \rangle^3 \langle v_n^2 \rangle \\ & + \langle v_m^6 v_k^2 \rangle - \langle v_m^6 \rangle \langle v_k^2 \rangle - 3 \langle v_m^2 v_k^2 \rangle \langle v_m^4 \rangle - 3 \langle v_m^4 v_k^2 \rangle \langle v_m^2 \rangle \\ & + 6 \langle v_m^4 \rangle \langle v_m^2 \rangle \langle v_k^2 \rangle + 6 \langle v_m^2 v_k^2 \rangle \langle v_m^2 \rangle^2 - 6 \langle v_m^2 \rangle^3 \langle v_k^2 \rangle \\ = & AC_{3,1}(m, n) + AC_{3,1}(m, k) \end{aligned} \quad (57)$$

387 After this demonstrations we can conclude that our estimator $AC_{3,1}(m, n)$ meets all
 388 the requirements for a cumulant. In the following section we will review its characteristic
 389 with a toy Monte Carlo simulation using our generic framework from chapter 2.

390 5 Toy Monte Carlo studies

391 Theoretically, the cumulant's value must be zero, when its variables are statistically inde-
 392 pendent (no genuine multi-body interaction). In our generic framework, We can see this
 393 if we take the values of flow amplitudes in Eq. (12) to solve Eq. (48). We will proceed to
 394 demonstrate this in another toy monte carlo simulation.

395 To illustrate this behavior, we first will introduce previous studies and then we will
 396 compare them with our own results. With the use of the realistic Monte Carlo (MC) event
 397 generator HIJING, Bilandzic et. al. have demonstrated the robustness of the proposed
 398 observables against few-particle nonflow correlations [13, 14, 12]. HIJING (for Heavy-Ion
 399 Jet Interaction Generator) is a combination of models describing jet and nuclear-related
 400 mechanisms, like jet production and fragmentation or nuclear shadowing to cite only a few.
 401 It is very useful for us, because it does not include any collective effects such as anisotropic
 402 flow, and because we want to study the sensitivity of a flow estimator against nonflow.

403 Figures (10 and 9) show the centrality dependence of our two-harmonic between dif-
 404 ferent moments of v_2^2 and v_4^2 , $AC_{3,1}(2, 4)$ and $AC_{2,1}(2, 4)$, respectively. This results were
 405 obtained in the paper [12]. Data from Pb-Pb collisions was simulated at a center-of-mass
 406 energy of $\sqrt{s_{NN}} = 2.76$ TeV. Two kinetic criteria have been applied as well: $0.2 < pT <$
 407 5.0 GeV/c and $|\eta| < 0.8$. The different correlators involved in the expression of $AC_{2,1}(2, 4)$

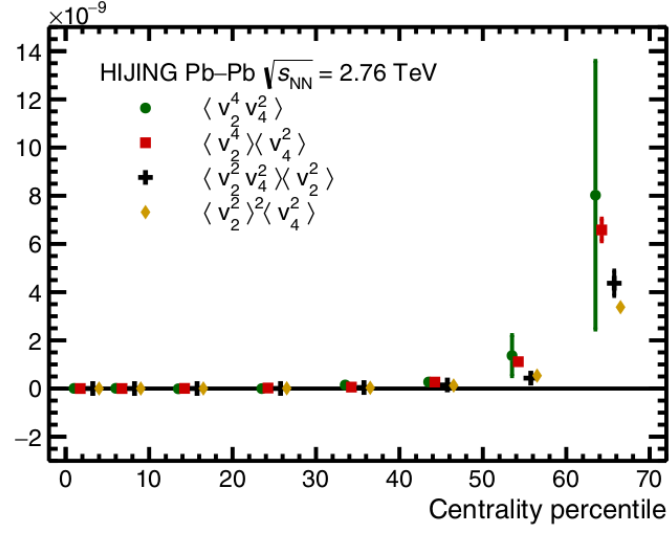


Figure 8: Centrality dependence of the correlators that are used in the calculus of our cumulants.

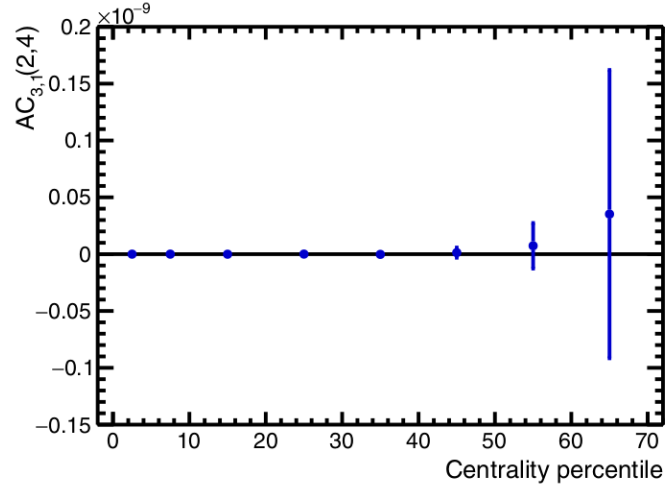


Figure 9: Centrality dependence of the correlator $AC_{3,1}(2,4)$.

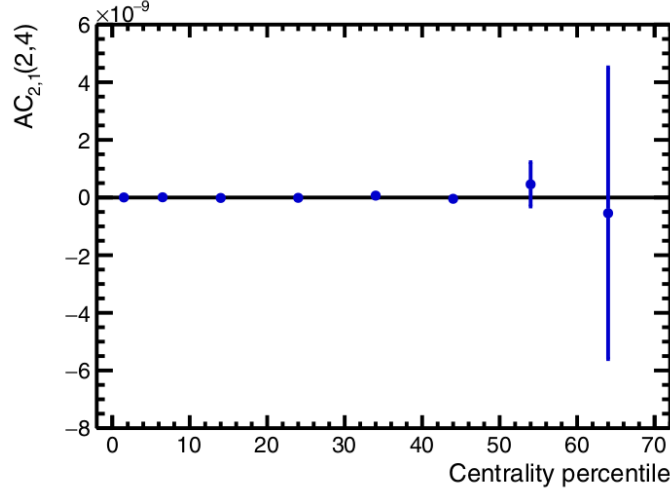


Figure 10: Centrality dependence of the correlator $AC_{2,1}(2,4)$.

are shown in Fig.(8). These two quantities are in agreement with zero for the full centrality range, meaning they are robust against few-particle nonflow correlations.

After introducing these studies we will now find the values of our cumulants $AC_{3,1}(2,4)$ and $AC_{2,1}(2,4)$. Experimentally, we can use estimators to calculate our ACs from the multiparticle correlations. We just need the Eq. (9) to eliminate any symmetry plane contribution, by setting zero to the sum of harmonics. These estimators have the following form (Eq. C6 and C7 from [12]):

$$\begin{aligned}
AC_{3,1}(m,n) = & \left\langle \left\langle e^{i(m\varphi_1+m\varphi_2+m\varphi_3+n\varphi_4-m\varphi_5-m\varphi_6-m\varphi_7-n\varphi_8)} \right\rangle \right\rangle \\
& - \left\langle \left\langle e^{i(m\varphi_1+m\varphi_2+m\varphi_3-m\varphi_4-m\varphi_5-m\varphi_6)} \right\rangle \right\rangle \left\langle \left\langle e^{i(n\varphi_1-n\varphi_2)} \right\rangle \right\rangle \\
& - 3 \left\langle \left\langle e^{i(m\varphi_1+m\varphi_2-m\varphi_3-m\varphi_4)} \right\rangle \right\rangle \left\langle \left\langle e^{i(m\varphi_1+n\varphi_2-m\varphi_3-n\varphi_4)} \right\rangle \right\rangle \\
& - 3 \left\langle \left\langle e^{i(m\varphi_1+m\varphi_2+n\varphi_3-m\varphi_4-m\varphi_5-n\varphi_6)} \right\rangle \right\rangle \left\langle \left\langle e^{i(m\varphi_1-m\varphi_2)} \right\rangle \right\rangle \\
& + 6 \left\langle \left\langle e^{i(m\varphi_1+m\varphi_2-m\varphi_3-m\varphi_4)} \right\rangle \right\rangle \left\langle \left\langle e^{i(m\varphi_1-m\varphi_2)} \right\rangle \right\rangle \left\langle \left\langle e^{i(n\varphi_1-n\varphi_2)} \right\rangle \right\rangle \\
& + 6 \left\langle \left\langle e^{i(m\varphi_1+n\varphi_2-m\varphi_3-n\varphi_4)} \right\rangle \right\rangle \left\langle \left\langle e^{i(m\varphi_1-m\varphi_2)} \right\rangle \right\rangle^2 \\
& - 6 \left\langle \left\langle e^{i(m\varphi_1-m\varphi_2)} \right\rangle \right\rangle^3 \left\langle \left\langle e^{i(n\varphi_1-n\varphi_2)} \right\rangle \right\rangle.
\end{aligned} \tag{58}$$

$$\begin{aligned}
AC_{2,1}(m,n) = & \left\langle \left\langle e^{i(m\varphi_1+m\varphi_2+n\varphi_3-m\varphi_4-m\varphi_5-n\varphi_6)} \right\rangle \right\rangle \\
& - \left\langle \left\langle e^{i(m\varphi_1+m\varphi_2-m\varphi_3-m\varphi_4)} \right\rangle \right\rangle \left\langle \left\langle e^{i(n\varphi_1-n\varphi_2)} \right\rangle \right\rangle \\
& - 2 \left\langle \left\langle e^{i(m\varphi_1+n\varphi_2-m\varphi_3-n\varphi_4)} \right\rangle \right\rangle \left\langle \left\langle e^{i(m\varphi_1-m\varphi_2)} \right\rangle \right\rangle \\
& + 2 \left\langle \left\langle e^{i(m\varphi_1-m\varphi_2)} \right\rangle \right\rangle^2 \left\langle \left\langle e^{i(n\varphi_1-n\varphi_2)} \right\rangle \right\rangle
\end{aligned} \tag{59}$$

Double angle parenthesis means that the code first gets the means in an event and then calculates the mean in all events. After this, we can recognize the correlators of Eq. (11).

type of distribution	average of $AC_{3,1}(2, 4)$	uncertainty
uniform acceptance	$5.761\,44 \times 10^{-10}$	$2.570\,64 \times 10^{-9}$
nouniform acceptance	$-3.606\,15 \times 10^{-8}$	1.6916×10^{-8}
nonuniform acceptance + φ -weights	$-8.077\,76 \times 10^{-10}$	1.6097×10^{-9}

Table 1: Results of the first Monte Carlo simulation for our proposed cumulant $AC_{3,1}(2, 4)$. We used azimuthal distribution from section 2; the application of weights corrects any biases. Only with a detector bias, the value of the cumulant $AC_{3,1}(2, 4)$ cannot be identically zero. This means, in this case, that there is a multi-body interaction.

type of distribution	average of $AC_{2,1}(2, 4)$	uncertainty
uniform acceptance	$-1.813\,16 \times 10^{-10}$	4.2044×10^{-9}
nouniform acceptance	$-6.731\,24 \times 10^{-7}$	$1.583\,83 \times 10^{-7}$
nonuniform acceptance + φ -weights	$5.475\,84 \times 10^{-10}$	$5.004\,23 \times 10^{-9}$

Table 2: Results of the second Monte Carlo simulation. Like previously, we used here the azimuthal distributions from section 2. The theoretical value for the cumulant $AC_{2,1}(2, 4)$ is near zero. Only with a detector bias, the value of the cumulant $AC_{3,1}(2, 4)$ cannot be identically zero. This means, in this case, that there is a multi-body interaction.

417 Like in previous studies we have selected $m = 2$ and $n = 4$. The cumulants become:

$$\begin{aligned}
AC_{3,1}(2, 4) = & \left\langle \langle 8 \rangle_{2,2,2,4,-2,-2,-2,-4} \right\rangle \\
& - \left\langle \langle 6 \rangle_{2,2,2,-2,-2,-2,-2} \right\rangle \left\langle \langle 2 \rangle_{4,-4} \right\rangle \\
& - 3 \left\langle \langle 4 \rangle_{2,2,-2,-2} \right\rangle \left\langle \langle 4 \rangle_{2,4,-2,-4} \right\rangle \\
& - 3 \left\langle \langle 6 \rangle_{2,2,4,-2,-2,4} \right\rangle \left\langle \langle 2 \rangle_{2,-2} \right\rangle \\
& + 6 \left\langle \langle 4 \rangle_{2,2,-2,-2} \right\rangle \left\langle \langle 2 \rangle_{2,-2} \right\rangle \left\langle \langle 2 \rangle_{4,-4} \right\rangle \\
& + 6 \left\langle \langle 4 \rangle_{2,4,-2,-4} \right\rangle \left\langle \langle 2 \rangle_{2,-2} \right\rangle^2 \\
& - 6 \left\langle \langle 2 \rangle_{2,-2} \right\rangle^3 \left\langle \langle 2 \rangle_{4,-4} \right\rangle
\end{aligned} \tag{60}$$

$$\begin{aligned}
AC_{2,1}(2, 4) = & \left\langle \langle 6 \rangle_{2,2,4,-2,-2,-4} \right\rangle \\
& - \left\langle \langle 4 \rangle_{2,2,-2,-2} \right\rangle \left\langle \langle 2 \rangle_{4,-4} \right\rangle \\
& - 2 \left\langle \langle 4 \rangle_{2,4,-2,-4} \right\rangle \left\langle \langle 2 \rangle_{2,-2} \right\rangle \\
& + 2 \left\langle \langle 2 \rangle_{2,-2} \right\rangle^2 \left\langle \langle 2 \rangle_{4,-4} \right\rangle
\end{aligned} \tag{61}$$

418 Figures (11) show the distribution used to obtain the azimuthal angles. Like in sec-
419 tion 2 we have here a bias in angles between 30° and 60° , they are 50% less probable to
420 appear. We used the weights from figure (12) to correct this bias. The tables (1) and (2)
421 shows the results of simulation for the estimators $AC_{3,1}(2, 4)$ and $AC_{2,1}(2, 4)$, respectively.

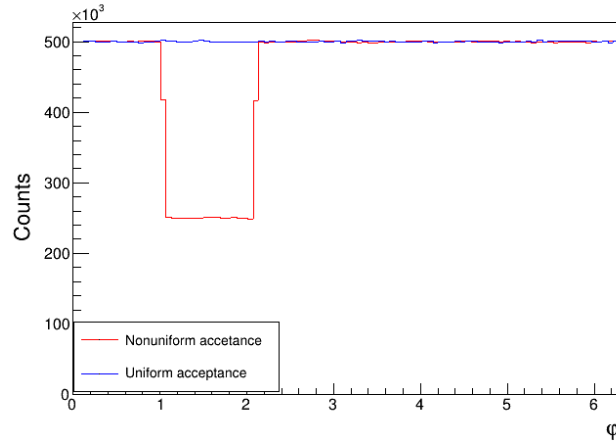


Figure 11: Azimuthal distributions for the monte carlo simulation. The red line represents a detector that has bias in angles between 30° and 60° .

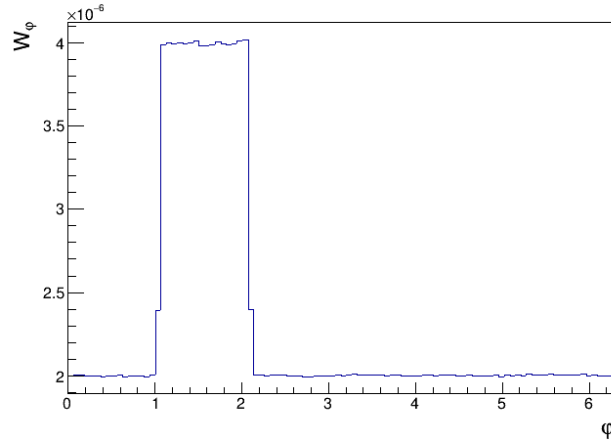


Figure 12: Weights obtained inverting the red histogram from Fig. (11). This corrects the azimuthal bias of the detector.

422 For the uniform acceptance and nonuniform acceptance + weights, their values are in or-
423 der of 10^{-10} . The respective uncertainties were calculated using the bootstrap technique
424 described in Appendix B. They are in the order of 10^{-9} and 10^{-7} , respectively. The theo-
425 retical value is zero, and it is located inside the accepted interval. This was totally expected
426 due to our estimators being a cumulant. In the case of the nonuniform acceptance, we see
427 that the accepted intervals does not include zero. This means, in this case, that there is a
428 multi-body interaction.

429 If we compare with previous studies, for $AC_{2,1}(2,4)$ From the figures (10) (9), we
430 can see that at least 55% of events have the values in our simulations from table (1) and
431 (2), respectively. Thus we have experimentally demonstrated that our estimators can be
432 classified as cumulants.

433 Appendix A Demonstrations

434 **A.1** $\langle \cos [n(\varphi - \Psi_n)] \rangle = v_n$

435 If we replace and calculate the following integral, we obtain the flow harmonics v_n :

$$\begin{aligned}
 \langle \cos [n(\varphi - \psi_n)] \rangle &= \int_0^{2\pi} \cos [n(\varphi - \psi_n)] \cdot f(\varphi) d\varphi \\
 &= \frac{1}{2\pi} \left[\int_0^{2\pi} \cos [n(\varphi - \psi_n)] d\varphi \right] \\
 &\quad + \frac{1}{\pi} \left[\sum_{m=1}^{\infty} v_m \int_0^{2\pi} \cos [n(\varphi - \psi_n)] \cdot \cos [m(\varphi - \psi_m)] d\varphi \right] \\
 &= \frac{1}{2\pi} \left[\int_0^{2\pi} \cos [n(\varphi - \psi_n)] d\varphi + 2 \sum_{m=1}^{\infty} v_m \pi \cos(\psi_n - \psi_m) \delta_{mn} \right] \\
 &= \frac{1}{2\pi} \left[\int_0^{2\pi} \cos [n(\varphi - \psi_n)] d\varphi + 2\pi v_n \right] = v_n
 \end{aligned} \tag{62}$$

436 The integral of the first term is zero:

$$\int_0^{2\pi} \cos [n(\varphi - \psi_n)] d\varphi = \int_0^{2\pi} (\cos(nx) \cos(n\psi_n) - \sin(nx) \sin(n\psi_n)) dx = 0 \tag{63}$$

437 **A.2** $\langle \cos [n(\varphi_1 - \varphi_2)] \rangle = v_n^2$

438 With the p.d.f from Eq. (2) and definition from Eq. (4) we obtain directly the result:

$$\begin{aligned}
 \langle \cos [n(\varphi_1 - \varphi_2)] \rangle &= \frac{1}{4\pi^2} \int_0^{2\pi} \int_0^{2\pi} d\varphi_1 d\varphi_2 \cos(n(\varphi_1 - \varphi_2)) \left[1 \right. \\
 &\quad + \sum_{p=1}^{\infty} v_p \cos(p(\varphi_1 - \psi_p)) \\
 &\quad + 2 \sum_{m=1}^{\infty} v_m \cos(m(\varphi_1 - \psi_m)) \\
 &\quad \left. + 4 \sum_{m=1}^{\infty} \sum_{p=1}^{\infty} v_p v_m \cos(m(\varphi_1 - \psi_m)) \cos(p(\varphi_2 - \psi_p)) \right]
 \end{aligned} \tag{64}$$

439 The first term is trivially similar to Eq. (63)

$$\int_0^{2\pi} \int_0^{2\pi} d\varphi_1 d\varphi_2 \cos(n(\varphi_1 - \varphi_2)) = 0 \tag{65}$$

440 The second term is zero. We use the orthogonality relation of trigonometric functions:

$$\begin{aligned}
 &2 \sum_m^{\infty} v_m \int_0^{2\pi} \int_0^{2\pi} d\varphi_1 d\varphi_2 \cos(m(\varphi_1 - \psi_m)) \cos(n(\varphi_1 - \varphi_2)) \\
 &= 2 \sum_m^{\infty} v_m \int_0^{2\pi} d\varphi_2 \int_0^{2\pi} d\varphi_1 \cos(m(\varphi_1 - \psi_m)) \cos(n(\varphi_1 - \varphi_2)) \\
 &= 2 \sum_m^{\infty} v_m \pi \int_0^{2\pi} d\varphi_2 \cos(m(\varphi_2 - \psi_m)) \delta_{mn} = 2v_n \pi \int_0^{2\pi} d\varphi_2 \cos(\varphi_2 - \psi_n) = 0
 \end{aligned} \tag{66}$$

```

4 Double_t bootstr(Double_t data[10000], Int_t N, Double_t mean0){
5 Double_t sum=0;
6 Int_t p=0;
7 Int_t n=10000/N; //number of entries per subsample
8 for (Int_t j=0;j<N;j++){
9     Double_t sumj=0, meanv2j=0;
10    for (Int_t s=0;s<n;s++){
11        p=j*n+s;
12        sumj=sumj+data[p];
13    }
14    meanv2j=sumj/n;
15    sum=sum+(meanv2j-mean0)*(meanv2j-mean0);
16 }
17 Double_t var=sum/(N-1);
18 Double_t uncertainty=sqrt(var/N);
19 return uncertainty;
20 }

```

Figure 13: Function to get the bootstrap uncertainty. Data was stored on array data. There were N subsamples and the variable mean0 is the mean of the original sample.

441 The third term is also zero, and for the last term we also use the orthogonality relations:

$$\begin{aligned}
 & 4 \sum_{p=1}^{\infty} \sum_{m=1}^{\infty} v_p v_m \int_0^{2\pi} d\varphi_2 \cos(p(\varphi_2 - \psi_p)) \int_0^{2\pi} d\varphi_1 \cos(m(\varphi_1 - \psi_m)) \cos(n(\varphi_1 - \varphi_2)) \\
 &= 4 \sum_{p=1}^{\infty} v_p \int_0^{2\pi} d\varphi_2 \cos(p(\varphi_2 - \psi_p)) \sum_{m=1}^{\infty} v_m \pi \cos(n\varphi_2 - m\varphi_m) \delta_{mn} \\
 &= 4\pi v_n \sum_{p=1}^{\infty} v_p \int_0^{2\pi} d\varphi_2 \cos(p(\varphi_2 - \psi_p)) \cos(n(\varphi_2 - \psi_n)) = 4\pi^2 \sum_{p=1}^{\infty} \cos(\psi_p - \psi_n) \delta_{pn} \\
 &= 4\pi^2 v_n^2.
 \end{aligned} \tag{67}$$

442 This give us the expected result v_n^2 .

443

444 A.3 Two particle correlation

445 In terms of the Q vector this can be expressed as:

$$\begin{aligned}
 \sum_{\substack{i,j=1 \\ (i \neq j)}}^M e^{in(\varphi_i - \varphi_j)} &= \sum_{i,j=1}^M e^{in(\varphi_i - \varphi_j)} - \sum_{i=j}^M e^{in(\varphi_i - \varphi_j)} = \sum_{i,j=1}^M e^{in(\varphi_i - \varphi_j)} - M \\
 &= \left(\sum_{i=1}^M e^{in\varphi_i} \right) \left(\sum_{j=1}^M e^{in\varphi_j} \right) - M = Q_n Q_n^* - M \\
 &= |Q_n|^2 - M
 \end{aligned} \tag{68}$$

446 Appendix B Bootstrap technique

447 The frequent problem after measuring an experiment, is finding the uncertainty. This
448 becomes even harder for compound observables. For instance, if the directly measured
449 observables are x and y , but we are looking for the quantity $z \equiv x^2 + e^{-y} + \cos xy$,
450 it is very difficult to perform the standard error propagation and obtain the statistical
451 uncertainty for desired observable z , from the statistical uncertainties of σ_x , σ_y and their

452 covariance $\text{Cov}(x, y)$, which can be obtained directly, because only x and y are measured
 453 like that. This sort of problem in general can be resolved with the bootstrap technique.
 454 In ALICE, physicists have endorsed the simplified version of bootstrap technique to find
 455 statistical uncertainties. The following steps must be done:

- 456 1. Divide the initial sample in 10 subsamples, so that each subsample contains roughly
 457 the same statistics;
- 458 2. For each subsample, perform an independent measurement and get for the observable
 459 of interest the results $\mu_0, \mu_1, \dots, \mu_9$, respectively;
- 460 3. Compute an unbiased variance from these 10 subsamples; i.e.

$$\text{Var} = \frac{1}{10-1} \sum_i^{10} (\mu_i - \mu)^2, \quad (69)$$

461 where the result for the starting large sample of the observable of interest is denoted
 462 by μ in the above formula.

- 463 4. The final result for observable of interest and its statistical uncertainty is:

$$\mu \pm \sqrt{\frac{\text{Var}}{10}}. \quad (70)$$

464 A function to get the uncertainty using this technique is shown in Fig. (13).

465 Appendix C Code to calculate the correlations

466 The main idea is shown in Fig. (14). In each event (in total nEvents), we uniformly extract
 467 the value of symmetry plane between the range 0 and 2π . Then, in line 569, we sample
 468 the angles (in total nAngles) from a distribution fvarphi, also Eq. (14). Between lines
 469 570 and 577, we calculate the detector's bias. Finally after line 585 we start to find the
 470 correlations and save their values in TProfile histograms. These will give us the averages
 471 and uncertainties.

```

561 //=====
562 //NONUNIFORM + Weights Filling
563 for (int t=0;t<nEvents;t++){ //events
564     fvarphi->SetParameter(0,gRandom->Uniform(TMath::TwoPi())); // sample randomly reaction plane
565
566 //Filling angles and weights
567     for(int r=0;r<nParticles;r++){ //particles
568         // Azimuthal angles:
569         angle=fvarphi->GetRandom();
570         while (angle > TMath::TwoPi()/6 && angle < TMath::TwoPi()/3){
571             if (gRandom->Uniform(0,1)<0.5){
572                 break;
573             }
574             else {
575                 angle=fvarphi->GetRandom();
576             }
577         }
578         angles[r]=angle;
579         //Find the corresponding weights
580         weights[r] = w->GetBinContent(w->FindBin(angles[r]));
581     }
582
583     //To do for each event:
584
585     bUseWeights = kTRUE;
586
587     // c) Calculate Q-vectors for available angles and weights;
588     CalculateQvectors();
589
590     // d) Calculate n-particle correlations from Q-vectors (using standalone formulas), and with t
591     // 2-p correlations:
592     TComplex two = Two(-2,2)/Two(0,0).Re();
593     Double_t wTwo = Two(0,0).Re(); // Weight is 'number of combinations' by default
594     nonuniformw[0][0]->Fill(0.5,two.Re(),wTwo); // <<cos(h1*phi1+h2*phi2)>>

```

Figure 14: Code to sample angles and calculate correlators from them.

References

- [1] Ryogo Kubo Journal of the Physical Society of Japan, 17, 1100-1120 (1962) 10.1143/JPSJ.17.1100
- [2] A. Bilandzic, CERN-THESIS-2012-018.
Direct link: https://www.nikhef.nl/pub/services/biblio/theses_pdf/thesis_A_Bilandzic.pdf
- [3] R. S. Bhalerao, M. Luzum and J. Y. Ollitrault, Phys. Rev. C **84** (2011) 034910 [arXiv:1104.4740 [nucl-th]].
- [4] A. Bilandzic, C. H. Christensen, K. Gulbrandsen, A. Hansen and Y. Zhou, Phys. Rev. C **89** (2014) 6, 064904 [arXiv:1312.3572 [nucl-ex]].
- [5] Bhalerao, Rajeev S. (2014). "Relativistic heavy-ion collisions". In Mulders, M.; Kawa-goe, K. (eds.). 1st Asia-Europe-Pacific School of High-Energy Physics. CERN Yellow Reports: School Proceedings. Vol. CERN-2014-001, KEK-Proceedings-2013-8. Geneva: CERN. pp. 219–239. doi:10.5170/CERN-2014-001. ISBN 9789290833994. OCLC 801745660. S2CID 119256218.
- [6] Annala, E., Gorda, T., Kurkela, A. et al. Evidence for quark-matter cores in massive neutron stars. Nat. Phys. 16, 907–910 (2020). <https://doi.org/10.1038/s41567-020-0914-9>
- [7] Z. Fodor, S.D. Katz. The phase diagram of quantum chromodynamics. [arXiv:0908.3341 [hep-ph]].

- 492 [8] Abbott, A. CERN claims first experimental creation of quark–gluon plasma. *Nature*
493 403, 581 (2000). <https://doi.org/10.1038/35001196>
- 494 [9] RHIC Scientists Serve Up 'Perfect' Liquid. <https://www.bnl.gov/newsroom/news.php?a=110303>
- 495 [10] N. Borghini, P. M. Dinh, and J.-Y. Ollitrault, *Phys. Rev. C* **63**, 054906 (2001).
496 <https://doi.org/10.1103/PhysRevC.63.054906>
- 497 [11] Ante Bilandzic, M. Lesch, C. Mordasini, and S. F. Taghavi, *Phys. Rev. C* **102**, 024907
498 (2020). <https://doi.org/10.1103/PhysRevC.102.024907>
- 499 [12] Ante Bilandzic, M. Lesch, C. Mordasini, and S. F. Taghavi, *Phys. Rev. C* **105**, 024912
500 (2022). <https://doi.org/10.1103/PhysRevC.105.024912>
- 501 [13] X.-N. Wang and M. Gyulassy, *Phys. Rev. D* **44**, 3501 (1991).
- 502 [14] M. Gyulassy and X.-N. Wang, *Comput. Phys. Commun.* **83**, 307 (1994).
- 503 [15] Piotr Nowakowski, Przemysław Rokita, Łukasz Graczykowski, *Computer Physics*
504 *Communications*, Vol 271, 2022, <https://doi.org/10.1016/j.cpc.2021.108206>